Available online at www.sciencedirect.com
ScienceDirect
Polymer Degradation and Stability 93 (2008) 983–989
Polymer Degradation and Stability
www.elsevier.com/locate/polydegstab

Degradation induced variation of LC transition of poly(*n*-undecyl isocyanate)

Bi-Zen Hsieh [a], Hung-Yi Chuang [a], Liang Chao [b], Ying-Jie Huang [c], Po-Hao Tseng [d], Tar-Hwa Hsieh [a], Yu-Kai Han [a], Ko-Shan Ho [a,*]

[a] *Department of Chemical and Materials Engineering, National Kaohsiung University of Applied Sciences, 415 Chien-Kuo Road, San-Ming District, Kaohsiung 80778, Taiwan*
[b] *Center for General Education, Technology and Science Institute of Northern Taiwan, Peito, Taipei 11202, Taiwan*
[c] *Institute of Nanotechnology, National Chiao Tung University, 1001, Ta Hsueh Road, Hsinchu, Taiwan*
[d] *Ming-Dao High School, 497, Section 1, Chung-San Road, Wu-Zi County, Taichung, Taiwan*

Received 11 December 2007; received in revised form 13 January 2008; accepted 21 January 2008
Available online 15 February 2008

Abstract

The first-order thermal transitions including side-chain melting, crystal-LC, biphasic chimney-like, and isotropic transitions of poly(*n*-undecyl isocyanate) (PUDIC) were investigated by varying its thermal history. After annealing at 140 °C for different periods of time, it leads to different degrees of backbiting degradation into *n*-undecyl isocyanurate trimer which behaves as a solvent for the rest non-degraded/rigid PUDIC to change into a lyotropic LC from thermotropic transition. Based on the degree of degradation, various amounts of trimers are present and the PUDIC demonstrates different types of thermal transitions found in DSC thermograms due to the variation of the non-degraded PUDIC concentration in solvent trimers. Finally, a phase diagram includes all types of crystallines, LC, and isotropic regions can be drawn according to the DSC thermograms.

Keywords: Liquid crystal transition; Poly(*n*-undecyl isocyanate); Degradation; Trimer

1. Introduction

Alkyl substituted rigid polymers have attained a great interest mainly due to their thermotropic or lyotropic liquid-crystalline behavior. The unsubstituted rigid polymers are infusible and insoluble because of their ordered structures and little space between the rods. In alkyl substituted rigid polymers, *n*-alkyl groups are covalently attached to the backbone. Due to the compulsion forces between the polar main chains and the non-polar side chains, these polymers are fusible at convenient temperatures and soluble in common organic solvents.

The crystallization of alkyl side chains in flexible polymers has been widely studied. For example, Levon and Kim [1,2] investigated the crystallization behavior of the alkylated polyacrylates and found the intercalating structure of the side chains.

Flory [3,4] constructed a chimney-like phase diagram that can describe the formation of both lyotropic and thermotropic LC transitions for rigid polymer solutions. It is confirmed by other researchers [5,6]. Polyalkylisocyanates were found to undergo either thermotropic LC or lyotropic LC [7–10] transitions depending on the treatments.

The backbiting type of degradation of polyalkylisocyanates has been found at high temperature and the cyclized/backbiting thermal degradation resulted in the isocyanurates (trimer) [11,12]. The aim of this investigation is to control the degree of backbiting degradation to produce various amounts of trimers by annealing at high temperatures, staying for different periods of time, which would induce a lyotropic LC transition with the degraded trimers which behaved like

* Corresponding author. Fax: +886 7 3814526x5122.
E-mail address: hks@cc.kuas.edu.tw (K.-S. Ho).

0141-3910/$ - see front matter © 2008 Elsevier Ltd. All rights reserved.
doi:10.1016/j.polymdegradstab.2008.01.032

solvents, except the common thermotropic LC transition of PUDIC. We will use DSC thermograms to indicate the temperatures and the presence or absence of side-chain crystallization, LC transition, LC–chimney transition for lyotropic LC, and finally isotropic transition for different annealing times at degradation temperature. And combining with the DSC thermograms, we can construct a phase diagram for PUDIC, revealing the formations of both the thermotropic and lyotropic transitions.

2. Experimental

2.1. Synthesis of monomers

Monomer was prepared as follows: 23 ml (0.1 mol) of distilled lauroyl chloride (Aldrich, ACS grade) was mixed with 8 g of sodium azide (0.12 mol, Aldrich) in 250 ml dry toluene (dried with sodium and followed by distillation) and refluxed overnight. The unreacted sodium azide and by-product sodium chloride were separated by vacuum distillation. A distillate with b.p. at 80–85 °C (vacuumed to 800 Pa) was collected with a yield of 29%.

2.2. Polymerization [13,14]

Dimethylformamide (DMF, Aldrich, ACS grade, 250 ml) was placed into a 500 ml three-necked flask with 1 g phosphorus pentoxide (P_2O_5) overnight and then distilled with a b.p. at 38 °C and 400 Pa. Sodium cyanide was dried in vacuum with P_2O_5 for 4 h and dissolved in dry DMF (in a 10 ml volumetric flask) to make a saturated solution. A 100 ml flask was dried on flame and inert gas (argon) was purged through the system. The temperature was kept at −36 °C by a dry ice/acetone bath. Thirty milliliters of DMF was then injected into the flask, and 10 min later, 1 ml of undecyl isocyanate. After 20 min one drop of the saturated sodium cyanide solution of DMF was injected into the batch, a white cluster of polymer suddenly appeared in the solution. Excess methanol was poured into the mixture to terminate the polymerization.

The polymer was isolated by filtration and 0.3 g of white powder was obtained. This product was further purified by dissolution in chloroform, precipitation by methanol and drying in vacuum. Poly(*n*-undecyl isocyanate) (PUDIC) (0.23 g) was obtained with a yield of 23%.

2.3. Characterization and measurement

2.3.1. Nuclear magnetic resonance (NMR)

^{1}H NMR spectrum for characterization of *n*-undecyl isocyanate was obtained in a deuterated chloroform solution using a Bruker MSL-300 spectrometer operated at 300 MHz. And PUDIC dissolved in the deuterated chloroform (conc. 1 mg/ml) was placed in an NMR tube. ^{13}C NMR spectra were recorded on a Varian Gemini 300 MHz NMR spectrometer. Chemical shifts were referenced to ^{13}C signals of the deuterated solvent.

2.3.2. Wide angled X-ray diffraction (WAXD)

A Phillips X-ray generator was used for the X-ray diffraction studies. The samples were cast on the slide or placed on the slide. The sample was exposed to Cu/Ni radiation with 45 kV and 35 mA from 2° to 40°, the exposure time, 50 s in every 0.04° was used for this experiment.

2.3.3. Thermogravimetric analysis (TGA)

Samples were subjected to thermogravimetric analysis by a TA SDT-2960 at 10 °C/min, under purging N_2.

2.3.4. Differential scanning calorimetry (DSC)

About 8 mg of neat or blended sample was subjected to DSC using TA-2920 and heated at 10 °C/min, in purging N_2.

2.3.5. Optical microscopy

A Nikon FII optical microscope was applied for the morphology studies. The temperature was controlled by a Mettler hot stage. The crystal structures were characterized under polarization.

3. Results and discussion

3.1. Characterization

^{1}H NMR spectrum of the synthesized monomers proved them to be *n*-undecyl isocyanate (Fig. 1), which possess four types of methylenes $-CH_2-$, and methyl $-CH_3$ groups of the *n*-undecyl chain as shown in the attached chemical structure. ^{13}C NMR spectra were used to characterize PUDIC in $CHCl_3$-*d*. The result is shown in Fig. 1. The resonance peaks of various carbons are illustrated in the attached chemical structures. The aliphatic carbon peaks of *n*-undecyl side chain can be seen around 10–40 ppm from Fig. 2 except the number one carbon whose absorption peak is over 40 ppm and not demonstrated in the spectrum.

3.2. WAXD patterns with various thermal histories

It is known that the hairy-rod structure of a rigid polymer with long alkyl side chains easily demonstrates a self-organized layer-to-layer structure with alkyl side chains interdigitized to each other and the layer-to-layer distance can be determined from the diffraction angles (2θ) around 2–5° in its WAXD pattern [15–19]. The non-polar hydrocarbon side chains were pushed away and extended from the polar backbones, resulting in an additional diffraction peak at lower angles. These peaks represent the layer-to-layer distance between PUDIC backbones that were separated by interdigitized *n*-undecyl groups. To characterize the possible structural variation of the layered structure of PUDIC, the X-ray diffraction patterns of PUDIC with various thermal histories were taken and shown in Fig. 3. The distances between the layers were calculated from the diffraction peak at $2\theta = 2.5°$ which is corresponding to 2.47 nm with interdigitized side chains illustrated in Scheme 2(a). When PUDIC was annealed at 50 °C for 20 min to melt the side-chain crystals, the layered structure

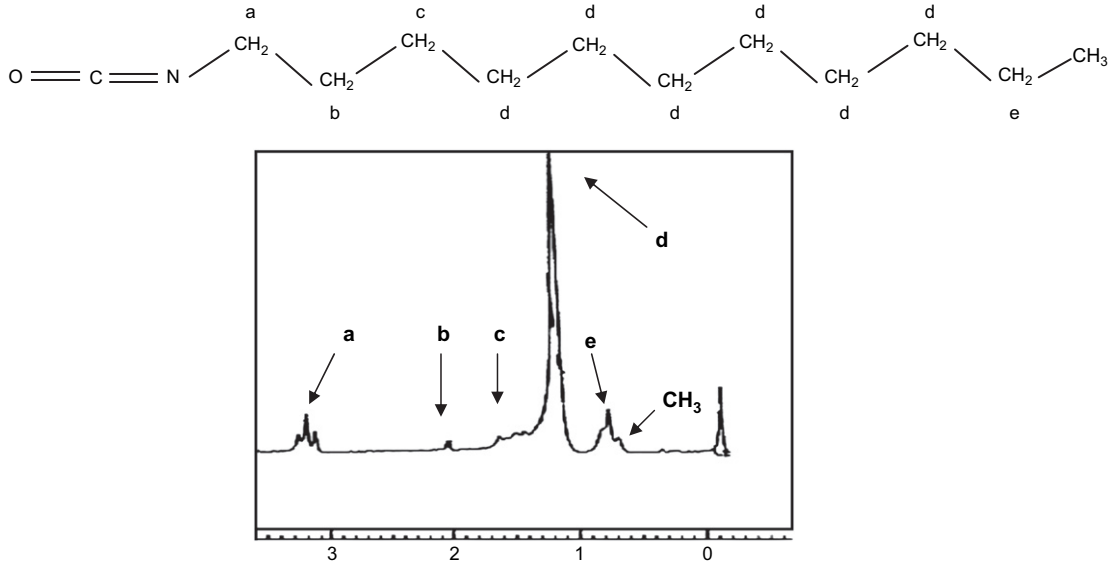

Fig. 1. ^{1}H NMR spectrum of *n*-undecyl isocyanate monomers.

was more significant as shown in Fig. 3(b) and Scheme 2(b) and the layer's distance remained the same indicating that the main crystalline structure of PUDIC was not destroyed with the melting of the side chains and no degradation phenomenon can be found with its X-ray diffraction pattern remaining almost the same with that of neat PUDIC. In Fig. 3(c) and Scheme 2(c) and (d), we found that the degradations werestrictly enhanced when the temperature was increased to 140 °C for 10 min and the X-ray diffraction patterns showed lots of sharp peaks in higher angles derived from the crystallization of the trimers (*n*-undecyl isocyanurates). These sharp peaks are contributed from the intercalated crystalline of the long hydrocarbon tails of the trimer molecules.

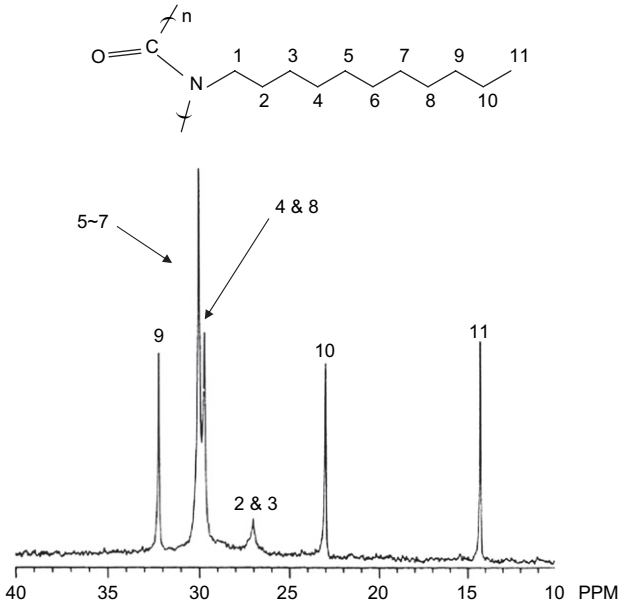

Fig. 2. ^{13}C NMR spectrum of PUDIC.

3.3. Thermal transitions and degradation

PUDIC was subjected to TGA to check its thermal degradation behavior. It seems very stable below 200 °C when the heating rate was maintained at 10 °C/min according to Fig. 4. However, the backbiting degradation of PUDIC (Scheme 1) causes no weight loss that cannot be illustrated by a TGA thermogram like Fig. 4. Actually, some fractal-like crystallines of the low molecular weight *n*-undecyl isocyanurate were already seen when PUDIC was annealed at 140 °C according to the polarized optical microscopic picture (POM) in Fig. 5. Therefore, the slight weight loss around 200 °C is more likely derived from the backbiting degradation of the PUDIC backbone and the plunging weight loss from 300 to 400 °C in Fig. 4 is the evaporation of the degradation product, trimers and other small fragments of PUDIC.

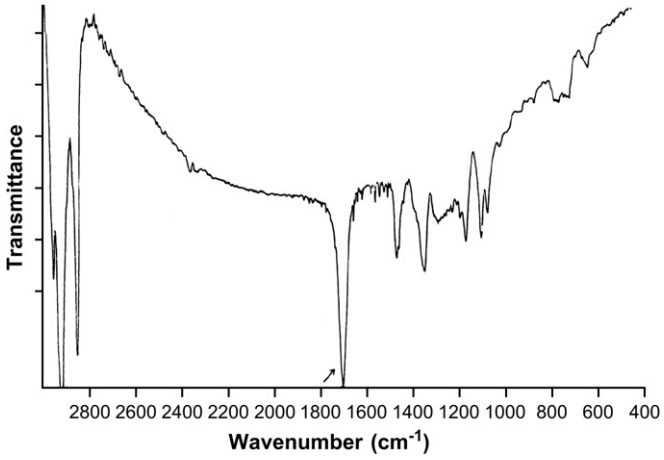

Fig. 3. Wide angled X-ray diffraction patterns of PUDIC with various thermal histories: (a) solvent cast; (b) 50 °C, 20 min and (c) 140 °C, 10 min.

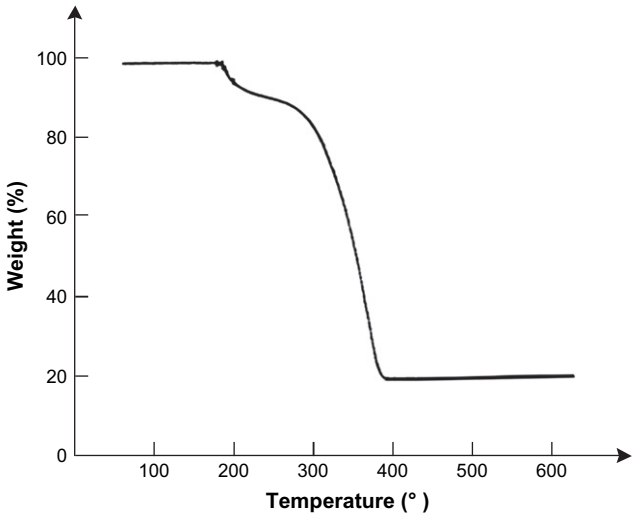

Fig. 4. TGA thermogram of PUDIC in N_2.

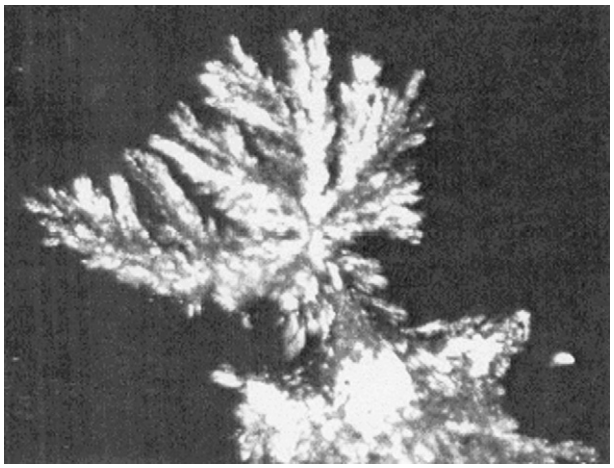

Fig. 5. POM picture with 200 × magnifications of crystallization of *n*-undecyl isocyanurate (trimer) at room temperature after annealing PUDIC at 140 °C for 10 min to indicate the presence of the unzipping degradation of PUDIC.

The DSC thermogram of PUDIC prepared from solvent casting is shown in Fig. 6(a) and all of the possible first-order thermal transitions of PUDIC were found and depicted in Scheme 2(a). It demonstrated first a well-defined layered 3D crystalline that is often found for most rigid polymers with long alkyl side chains with the main chains built into a 3D structure and alkyl side chains extended out from the backbones, interdigitizing into another zigzag-like crystalline structure.

The interdigitized side chains contributed to the lowest melting point as shown in Fig. 6(a). The melted side chains could provide necessary mobility and behave as lubricants when the 3D structure of PUDIC transformed into the 2D thermotropic (nematic) LC as illustrated in the POM picture in Fig. 7. However, if PUDIC has been annealed at high temperature, such as 140 °C, it could go on backbiting unzipping degrading into *n*-undecyl isocyanurates and the type of LC transition can be varied into a lyotropic LC transition, which is a rigid rod polymer dissolving in solvent (*n*-undecyl isocyanurates), before it went into the isotropic region. In other words, PUDIC with high temperature history can demonstrate a lyotropic LC when the degradation products, trimers have already melted at high temperatures and behave as solvents to create a biphasic chimney-like transition derived by Flory [3,4] which can be seen with double transitions at 100 and 120 °C in the DSC thermograms of Fig. 6(a) and (b).

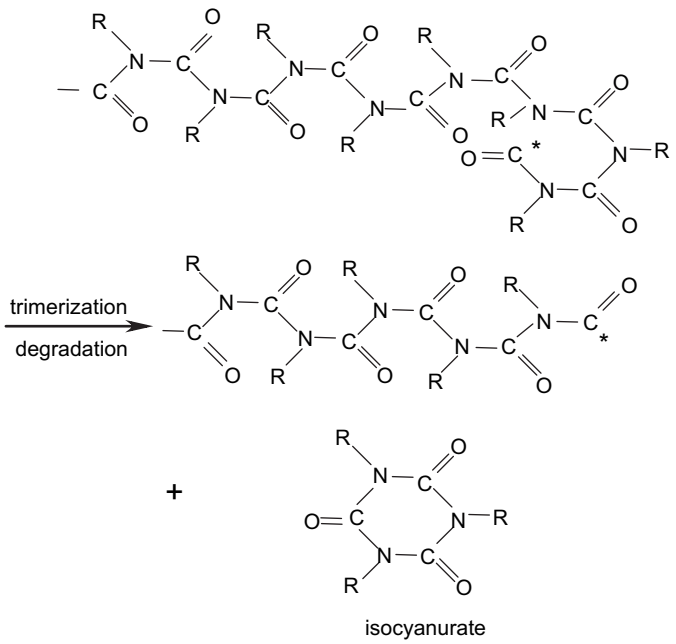

Scheme 1. Thermal degradation mechanism of PUDIC.

3.4. Possible phase diagram with degradation

The presence of these transitions illustrated in Scheme 2 was further confirmed by their DSC thermograms that were

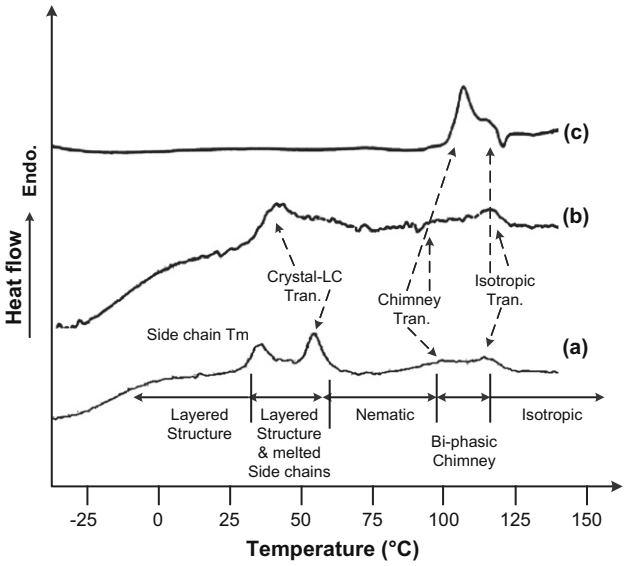

Fig. 6. (a) Solvent-cast PUDIC; PUDIC annealed at 140 °C for (b) 5 min (c) 10 min.

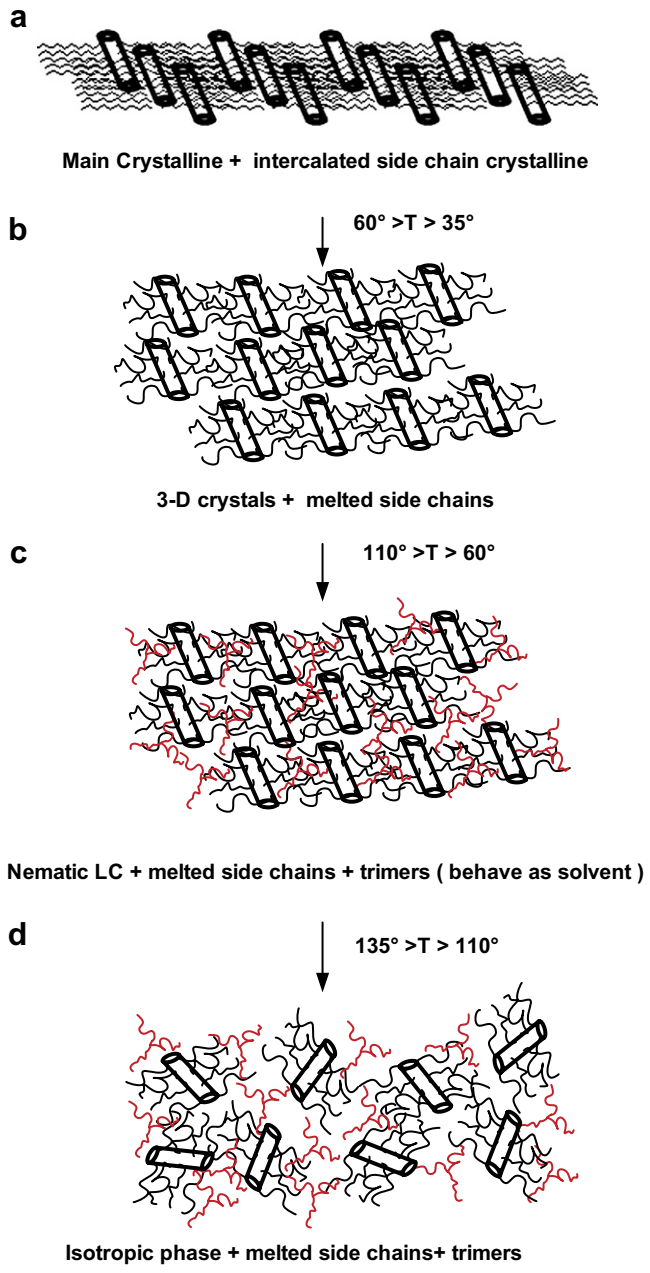

Scheme 2. Sketched thermal transitions of PUDIC (a) solvent-cast PUDIC and (b)–(d) after annealing at 140 °C, 5 min.

taken for PUDIC with various thermal histories depicted in Fig. 6. These DSC thermograms were used to draw a possible phase diagram including all possible thermal transitions as shown in Scheme 3. In Scheme 3(a), all transitions described in Scheme 2 were clearly seen in the DSC thermogram for the neat solvent-cast (*n*-hexane) PUDIC. There are side-chain melting at arround 30 °C, 3D to 2D nematic LC at 55 °C, nematic to biphasic/chimney-like lyotropic LC at 100 °C, and isotropic transition at 120 °C characterized from Fig. 6(a). Since there is no thermal history for the neat, solvent-cast PUDIC, we can assume that it followed the common thermotropic transitions for regular alkylated polyisocyanates below 100 °C. However, in the presence of the biphasic/chimney-like

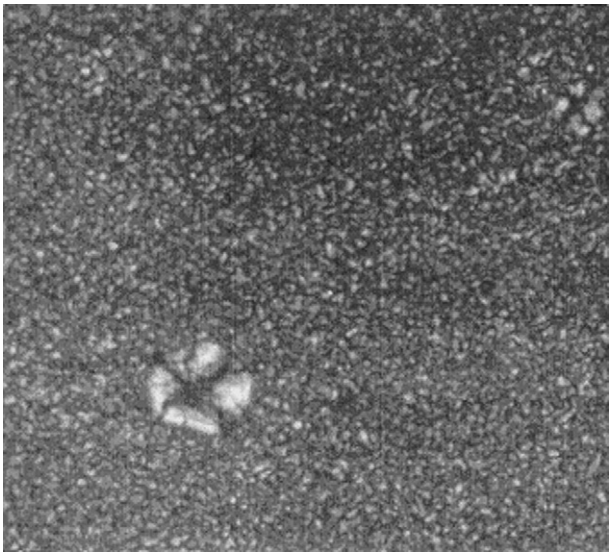

Fig. 7. POM picture with 200 magnifications of neat PUDIC nematic LC taken at 80 °C.

transition, we can understand the occurrence of the backbiting unzipping degradation of PUDIC (Scheme 1), which has been confirmed by Refs. [11,12]. Interestingly, the side-chain crystallization was not able to interdigitize into crystals after PUDIC was annealed at 140 °C for 5 min due to the interference of the degradation products, alkyl isocyanurate trimers that would then behave as solvents at high temperature. Therefore, the phase diagram should be moved forward to the lower concentration with more solvents/trimers created with annealing, resulting in the missing of the side-chain crystalline region as described in Scheme 3(b). However, the main crystalline (3D) and the thermotropic and lyotropic LC transitions can still be found in Fig. 6(b) and Scheme 3(b). Finally, if it stayed at 140 °C for longer time, the concentration goes lower and the phase diagram comes forward to a region beyond the main-chain (3D) crystalline. In other words, there is only 2D/nematic LC present at this stage and no 3D/2D transition can be found for the thermogram as illustrated in Fig. 6(c) and Scheme 3(c). Still, both the lyotropic LC and isotropic transitions are shown in Scheme 3(c). Since the degradation goes on rapidly after annealing at 140 °C for over 10 min, we were not able to find out rest of the transitions that are depicted in the phase diagram. Surprisingly, a special phase diagram including side-chain crystalline, main-chain/layered crystalline, thermotropic nematic LC transition, lyotropic LC transition, and isotropic region of PUDIC, accompanied with thermal degradation can be drawn.

4. Conclusions

Liquid-crystalline polymers especially alkyl side-chain polymers where additional crystallization may occur, should be characterized only with a controlled thermal history.

We have shown that the structure of polyalkylisocyanate depends greatly on previous history. The main-chain crystals

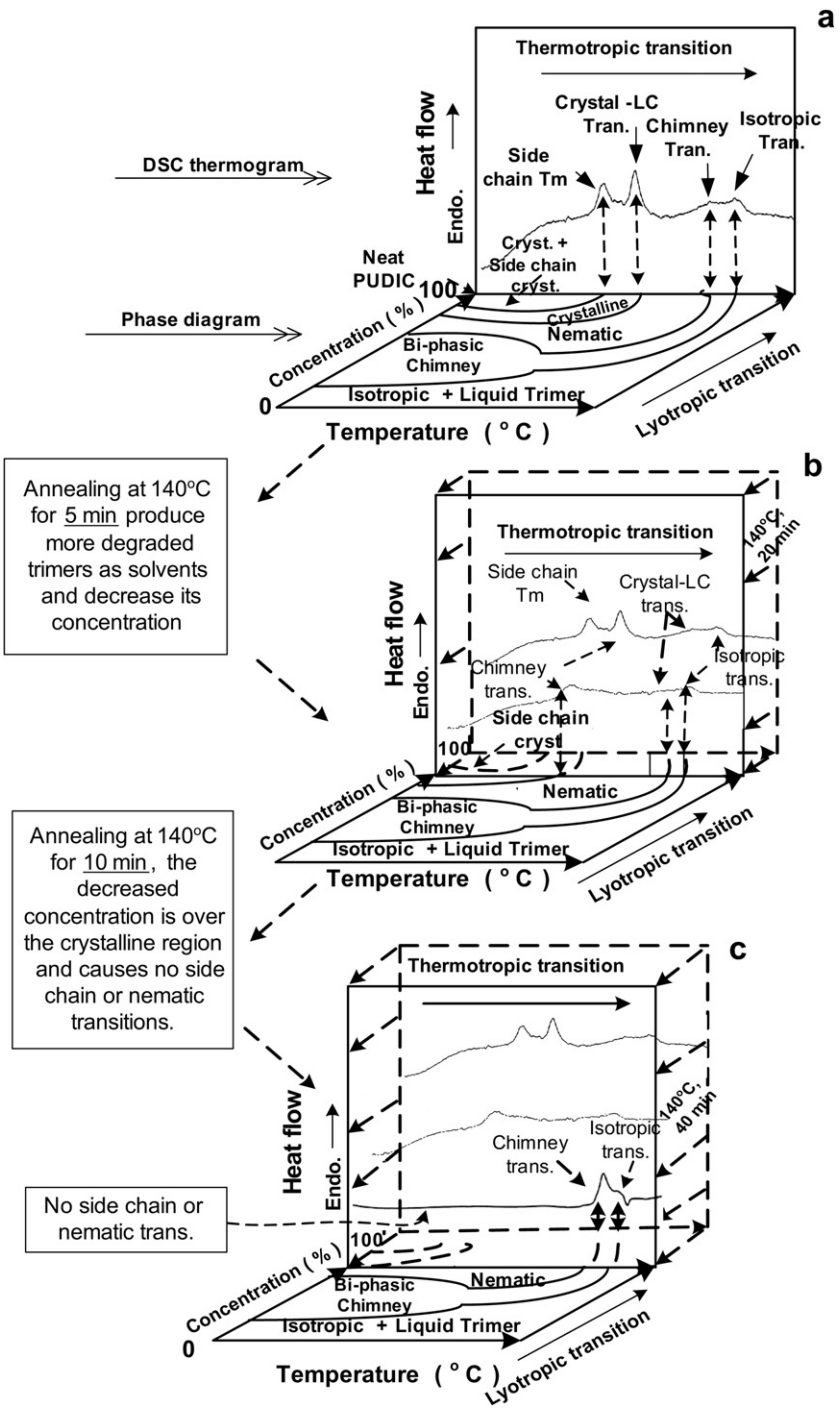

Scheme 3. Phase diagram of LC transition of PUDIC from DSC thermograms.

may be the only form of order but can exist alsowith side-chain crystals. It would be interesting to follow the kinetics of side-chain and main-chain crystallization from the liquid crystal as well as the isotropic phase.

There are several possible transitions that can be found by DSC thermograms and these transitions resulted from a phase diagram including side-chain crystal, main crystal, nematic (thermotropic), lyotropic, and isotropic regions accompanied with thermal/unzipping degradation of PUDIC. The phase diagram can be briefly drawn from the transitional temperatures of DSC thermograms taken for PUDIC with various thermal histories.

References

[1] Kim MS, Levon K. Blend of electroactive complexes of polyaniline and surfactant with alkylated polyacrylate. Journal of Colloid and Interface Science 1997;190:17–36.

[2] Kim MS, Levon K. Crystallization and phase separation of high-density polyethylene in the presence of comb-like polymer, poly(octadecyl acrylate). European Polymer Journal 1997;33:1787–98.

[3] Flory PJ. Statistical thermodynamics of mixtures of rodlike particles. 5. Mixtures with random coils. Macromolecules 1978;11:1138–41.
[4] Flory PJ. Statistical thermodynamics of mixtures of rodlike particles. 6. Rods connected by flexible joints. Macromolecules 1978;11:1141–4.
[5] Huber AE, Stayton PS, Viney C, Kaplan DL. Liquid crystallinity of a biological polysaccharide: the levan/water phase diagram. Macromolecules 1994;27:953–7.
[6] Viney C, Yoon DY, Reck B, Ringsdorf H. Phase behavior of a semiflexible polymer with both thermotropic and lyotropic properties. Macromolecules 1989;22:4088–93.
[7] Selinger JV, Selinger RLB, Jha SK, Green MMA. Chiral polymeric analogy to a one-dimensional paramagnetic material. Chirality 1998;10:41–5.
[8] Zhao WY, Kloczkowski A, Mark JE, Erman B, Bahar I. Main-chain lyotropic liquid-crystalline elastomers. 2. Orientation and mechanical properties of polyisocyanate films. Macromolecules 1996;29:2805–12.
[9] Seurin MJ, Bosch AT, Sixou P. Phase studies of a liquid crystalline polymer: hydroxypropyl cellulose. Polymer Bulletin 1983;10:450–6.
[10] Menna TJ, Filisko FE. Response of a biphasic poly(*n*-hexyl isocyanate)/*p*-xylene solution to applied high electric fields. Journal of Polymer Science, Part B: Polymer Physics 2005;43:1124–33.
[11] Backus K, Bernard DL, Darr WC, Saunders JH. Flammability and thermal stability of isocyanate-based polymers. Journal of Applied Polymer Science 1968;12:1053–74.
[12] Vazaios A, Pitsikalis M, Hadjichristidis N. Triblock copolymers and pentablock terpolymers of *n*-hexyl isocyanate with styrene and isoprene: synthesis, characterization, and thermal properties. Journal of Polymer Science, Part A-1: Polymer Chemistry 2003;41:3094–102.
[13] Koeckelberghs G, Beylan MV, Samyn C. Synthesis of new polyisocyanates. Materials Science and Engineering, C 2001;18:15–20.
[14] Koeckelberghs G, Beylan MV, Samyn C. Synthesis of new polyisocyanates. European Polymer Journal 2001;37:1991–6.
[15] Stepanyan R, Subbotin A, Knaapila M, Ikkala O, ten Brinke G. Self-organization of hairy-rod polymers. Macromolecules 2003;36:3758–63.
[16] Levon K, Ho KS, Zheng WY, Laakso J, Karna T, Taka T, et al. Thermal doping of polyaniline with dodecylbenzene sulfonic acid without auxiliary solvents. Polymer 1995;36:2733–8.
[17] Ho KS. Effects of phenolic based polymeric secondary dopants on polyaniline. Synthetic Metals 2002;26:151–8.
[18] Ho KS, Hsieh TH, Kuo CW, Lee SW, Lin JJ, Huang YJ. Effect of aniline formaldehyde resin on the conjugation length and structure of doped polyaniline: spectral studies. Journal of Polymer Science, Part A: Polymer Chemistry 2005;43:3116–25.
[19] Ho KS, Hsieh TH, Kuo CW, Lee SW, Huang YJ, Chuang CN. Effect of aniline formaldehyde resin on the reduced conjugation length of doped polyaniline: thermal studies. Journal of Applied Polymer Science 2006;12:773–81.